Remote Sensing of Arctic Vegetation: Relations between the NDVI, Spatial Resolution and Vegetation Cover on Boothia Peninsula, Nunavut

GITA J. LAIDLER,[1] PAUL M. TREITZ[2] and DAVID M. ATKINSON[2]

ABSTRACT. Arctic tundra environments are thought to be particularly sensitive to changes in climate, whereby alterations in ecosystem functioning are likely to be expressed through shifts in vegetation phenology, species composition, and net ecosystem productivity (NEP). Remote sensing has shown potential as a tool to quantify and monitor biophysical variables over space and through time. This study explores the relationship between the normalized difference vegetation index (NDVI) and percent-vegetation cover in a tundra environment, where variations in soil moisture, exposed soil, and gravel till have significant influence on spectral response, and hence, on the characterization of vegetation communities. IKONOS multispectral data (4 m spatial resolution) and Landsat 7 ETM+ data (30 m spatial resolution) were collected for a study area in the Lord Lindsay River watershed on Boothia Peninsula, Nunavut. In conjunction with image acquisition, percent cover data were collected for twelve 100 m × 100 m study plots to determine vegetation community composition. Strong correlations were found for NDVI values calculated with surface and satellite sensors, across the sample plots. In addition, results suggest that percent cover is highly correlated with the NDVI, thereby indicating strong potential for modeling percent cover variations over the region. These percent cover variations are closely related to moisture regime, particularly in areas of high moisture (e.g., water-tracks). These results are important given that improved mapping of Arctic vegetation and associated biophysical variables is needed to monitor environmental change.

Key words: tundra, biophysical remote sensing, vegetation indices, NDVI, percent cover, Landsat 7 ETM+, IKONOS, Boothia Peninsula, Canadian Arctic

RÉSUMÉ. On croit que les environnements de la toundra arctique sont particulièrement sensibles aux changements climatiques, en ce sens que toute altération du fonctionnement de l'écosystème est susceptible d'être exprimée dans le réarrangement de la phénologie de la végétation, de la composition des espèces et de la productivité nette de l'écosystème (PNÉ). La télédétection s'avère un outil efficace de quantification et de surveillance des variables biophysiques dans le temps et dans l'espace. Cette étude explore la relation entre l'indice d'activité végétale et le pourcentage de couverture végétale en milieu de toundra, où les variations propres à l'humidité du sol, au sol exposé et au till de gravier ont une influence considérable sur la réponse spectrale et, par conséquent, sur la caractérisation des communautés végétales. Des données multispectrales IKONOS (résolution spatiale de 4 m) et des données ETM+ de Landsat 7 (résolution spatiale de 30 m) ont été recueillies pour une zone d'étude visée par la ligne de partage des eaux à la hauteur de la rivière Lord Lindsay, dans la péninsule de Boothia, au Nunavut. De concert avec l'acquisition d'images, les données relatives au pourcentage de couverture ont été recueillies pour douze terrains d'étude de 100 m sur 100 m dans le but de déterminer la composition de la communauté végétale. De fortes corrélations ont été dénotées dans le cas des valeurs de l'indice d'activité végétale calculées à l'aide de détecteurs de surface et de détecteurs satellisés et ce, à l'échelle des terrains ayant servi d'échantillon. Par ailleurs, les résultats laissent entendre que le pourcentage de couverture est hautement corrélé avec l'indice d'activité végétale, ce qui indique une forte possibilité de modélisation des variations de pourcentage de couverture dans la région. Ces variations du pourcentage de couverture sont étroitement liées au régime d'humidité, particulièrement dans les régions où l'humidité est élevée (comme les traces d'eau). Ces résultats revêtent de l'importance étant donné qu'il y a lieu d'améliorer le mappage de la végétation arctique et les variables biophysiques connexes afin de surveiller la modification de l'environnement.

Mots clés : toundra, télédétection biophysique, indices de végétation, indices d'activité végétale, pourcentage de couverture, ETM+ de Landsat 7, IKONOS, péninsule de Boothia, Arctique canadien

Traduit pour la revue *Arctic* par Nicole Giguère.

[1] Department of Geography, University of Toronto, 100 St. George Street, Toronto, Ontario M5S 3G3, Canada; gita.laidler@utoronto.ca

[2] Department of Geography, D201 Mackintosh-Corry Hall, Queen's University, Kingston, Ontario K7L 3N6, Canada

INTRODUCTION

Tundra vegetation covers approximately six million square kilometers of the earth's surface and is thus an important consideration within the context of global climate change (Hope et al., 1993; Stow et al., 2004; Walker et al., 2005). Global climate change threatens to alter the climatic systems that have dominated Arctic latitudes for centuries (Serreze et al., 2000), and while tundra environments are thought to be particularly sensitive to such changes, how they will respond remains unclear (McMichael et al., 1999; Muller et al., 1999; Walker, 2000; Stow et al., 2004). On the basis of general circulation models (GCMs), it is predicted that Arctic mean annual temperatures will increase significantly in comparison to the global mean annual warming, thereby greatly affecting permafrost—the dominant control over tundra ecosystem processes (Hope et al., 1995). In fact, this temperature trend has been observed in the Arctic over the past 50 years (Hansen et al., 2005). This increase in temperature may lead to a release of previously sequestered carbon to the atmosphere, potentially shifting the global carbon budget because of the vast spatial extent of tundra environments (Vierling et al., 1997; Loya and Grogan, 2004; Walker et al., 2005). Further, climate change will not be uniform across the Arctic, but will demonstrate regional differences that will also foster corresponding changes in ecosystem function and vegetation response (Hansen et al., 1999; Stow et al., 2004).

Alterations to tundra ecosystem functioning are likely to be expressed through shifts in vegetation phenology, species composition, and net ecosystem productivity (NEP). Remote sensing may provide a viable way to monitor (and quantify) these changes. However, tundra environments pose significant challenges to the estimation of biophysical variables. First, Arctic landscapes are characterized by multiple scales of spatial heterogeneity (McFadden et al., 1998; Stow et al., 2004). Accounting for these spatial variations is difficult in remote sensing studies, in particular within the context of designing appropriate sampling strategies. Arctic regions such as coastal plains, polar deserts, or Arctic foothills are defined by climatic and hydrological influences, and they may extend over hundreds of kilometres. Each region may be deemed a mosaic, where vegetation types are found at scales ranging from 100 m to 1 km, while microsite variations (e.g., changes in relief due to hummocks and frost action in tussock tundra) may occur within centimetres to metres (McFadden et al., 1998). Second, small-scale vegetation studies may be ideal, but the harsh Arctic climate and the remote nature of field sites do not always render such studies feasible (Shippert et al., 1995; Jacobsen and Hansen, 1999), nor are they necessarily useful in extrapolating to broader expanses of land (Dungan, 1998; Lobo et al., 1998; Ostendorf and Reynolds, 1998; Davidson and Csillag, 2001). Remote sensing provides the potential to characterize surface variables that control carbon fluxes over landscapes (i.e., $100 \, m^2$ to $100 \, km^2$) or regions (i.e., $> 100 \, km^2$) (Hope et al., 1995). This capability is especially important in Arctic environments, where field studies are limited as a function of accessibility, financial cost, and weather conditions (Lévesque, 1996; Jacobsen and Hansen, 1999; Gould et al., 2003).

The unique spectral characteristics of vegetation are what make biophysical remote sensing possible. Vegetation, because of its chemical and structural characteristics, absorbs, reflects, and transmits electromagnetic radiation in a very different manner than other natural and anthropogenic surfaces. The contrast between chlorophyll absorption of visible wavelengths and strong reflectance in the near infrared (NIR) aid in discriminating plant types and have resulted in the development of numerous vegetation indices (VIs) that provide a means of quantitatively measuring certain biophysical parameters (Laidler and Treitz, 2003; Jensen, 2007). The catalyst to understanding biophysical trends using remote sensing data is the investigation of relationships between spectral vegetation indices, how they vary across landscapes, and how these fluctuations are related to vegetation composition, biomass, and ecological site factors (Walker et al., 1995; Boelman et al., 2003).

Vegetation indices are mathematical derivatives of spectral reflectance that are designed to provide a single value representative of the amount or vigour of vegetation within a pixel. They are generally less sensitive to external variables (e.g., solar zenith angle) than individual image channels (Laidler and Treitz, 2003; Jensen, 2007). The normalized difference vegetation index (NDVI; Rouse et al., 1974) is one of the most widely used. Within Arctic vegetation studies, it has been used at regional (Walker et al., 2002; Jia et al., 2003) and local scales (Shippert et al., 1995; Rees et al., 1998; McMichael et al., 1999).

In 2001, a field study was initiated on the Boothia Peninsula (Nunavut, Canada) to determine the relationship between percent cover of Arctic vegetation and spectral reflectance. The first objective of this study was to relate spectral vegetation indices (i.e., NDVI), as derived from remotely sensed data, to percent cover of Arctic vegetation. The second was to examine the effect of spatial resolution, or measurement scale, on the characterization of percent cover of tundra vegetation communities, thereby determining suitable scales at which to estimate vegetation communities that are highly spatially variable.

METHODS

Study Site Description

The study site is located on the Boothia Peninsula, in the Kitikmeot Region of Nunavut, within the Lord Lindsay River watershed, just west of Sanagak Lake (70°11′ N, 93°44′ W; Fig. 1). The Boothia Peninsula consists of extensive plateaus, plains, and lowlands, and the Boothia Plateau exhibits low, rolling bedrock hills with summits up to 500 m above sea level (Dyke, 1984). The landscape is underlain by crystalline gneiss forming a narrow north-trending prong of
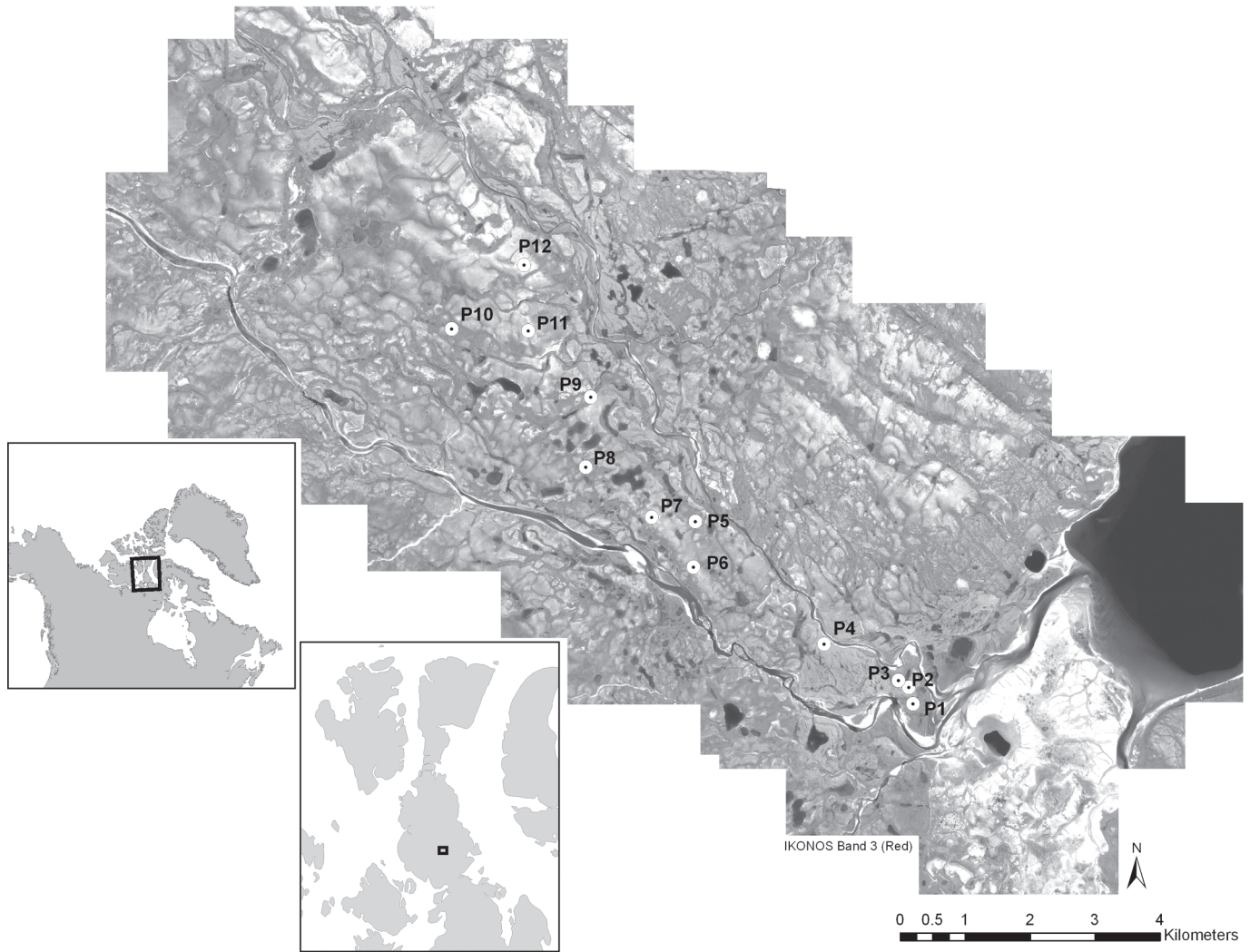
FIG. 1. Maps showing the study area location on Boothia Peninsula, Nunavut. The mosaic of IKONOS imagery (Band 3 – red wavelengths) shows the study area coverage, including the 12 study plots (P1 to P12).

the Precambrian Shield, partly covered by outliers of Palaeozoic strata (Environment Canada, 2000).

Arctic tundra vegetation comprises a mosaic of plant communities, usually compact, wind-sculptured, and less than one metre in height (Stonehouse, 1989). Lichens and mosses are prominent growth forms, but tundra communities also include shrubs, sedges, grasses, and forbs (flowering herbs other than grasses). Community composition varies in relation to soil quality, topography (i.e., slope, aspect, and elevation), duration of snow cover, and other variables. The study area falls within the prostrate dwarf-shrub (Arctic Tundra) sub-zone described by Walker et al. (2005). Characteristic of a mid-Arctic ecoclimate, vegetation on the peninsula is discontinuous, generally dominated by tundra species such as *Saxifraga oppositifolia*, *Dryas integrifolia*, and *Salix* spp. Wet areas have a continuous cover of sedges, (e.g., *Eriophorum* spp., *Saxifraga* spp.) and mosses. Over the broad study area, non-sorted circles, stripes, and ice-wedge polygons are abundant and frequently interrupt plant cover. Vascular vegetation is

often restricted to protected habitats, such as cracks and depressions in the polygon network and areas irrigated by runoff from snow patches (Walker, 2000). Prostrate and hemiprostrate dwarf shrubs (< 10 cm) are the dominant growth form on dry and mesic sites, whereas graminoids are more prominent on wet sites.

No long-term climate data are available for this study site. However, the Boothia Peninsula is located south of Resolute Bay and northeast of Cambridge Bay, so these two Nunavut communities provide the nearest meteorological stations with climate normals for 1971 – 2000 calculated using World Meteorological Organization standards. The mean annual temperature is -16.4°C for Resolute Bay and -14.4°C for Cambridge Bay, and their mean July temperatures are 4.3°C and 8.4°C (Environment Canada, 2004). Annual precipitation is approximately 150 mm for Resolute Bay and 138.8 mm for Cambridge Bay (Environment Canada, 2004).

A meteorological station was installed at the study site in 2001. During the two-week vegetation sampling period

(15 July to 8 August 2001), the site had a mean daily temperature of 14˚C with 0 mm of precipitation (Forbes, 2003).

Field Data Collection

Plot location, percent cover sampling, and spectral data collection occurred during the period from 15 June to 8 August 2001. An unsupervised spectral classification was used along with in situ visual identification to locate vegetation community types. Representative sample plots (i.e., 100 m × 100 m; 1 ha) were established for each vegetation community type. This large plot dimension was necessary for the accurate location of the selected areas on the coarsest resolution satellite imagery (i.e., Landsat 7 ETM+, 30 m pixels). Twelve plots (P1 to P12) were established for intensive study, and the corners and center of each plot were georeferenced (using a Trimble GeoExplorer II Global Positioning System [GPS]) for ease of identification on satellite imagery. The rationale for establishing 12 sample plots included i) a limited sampling window to capture peak seasonal growth patterns; ii) the intensity and duration of within-plot quadrat sampling; and iii) travel time and distance to remote plot locations.

Each 1 ha plot was divided into quadrants and then a total of 50 quadrats (50 cm × 50 cm; 0.25 m²) were sampled (12 quadrats in each of two quadrants, 13 quadrats in each of two quadrants), using a stratified random sampling technique without replacement. These quadrat dimensions represent the scale at which local heterogeneity is noticeable, although the same quadrats in combination give a homogeneous spectral response in satellite imagery at the scale of the whole plot. The Braun-Blanquet cover-class method was adopted for estimating the percentage of vegetation cover (percent cover) in each quadrat (Barbour et al., 1987). Individual plant species were documented to record species diversity, but percent cover was evaluated according to plant functional type (i.e., graminoids, forbs, shrubs, and bryophytes) to provide insight into community composition (after Walker, 2000), as well as for ease and accuracy in presenting results. These 50 quadrat estimates were later converted to plot-level percent cover values using the mean percent cover of each plant functional type, along with the mean percent of non-vegetated cover. In addition, 10 quadrats in each plot (i.e., every fifth quadrat) were sampled for relative soil moisture (after Edwards et al., 2000) (Table 1) and converted to plot-level moisture estimates using the median value. This characterization was useful in organizing graphic and statistical trends along a moisture gradient (i.e., driest to wettest), representing results according to an environmental parameter that affects percent cover and community type.

A portable FieldSpec® Pro spectro-radiometer (Analytical Spectral Devices, Boulder, CO) was used for all surface radiometric measurements. The FieldSpec Pro collects surface spectra across the wavelength range of 350–2500 nm, with sampling intervals of 1.4 nm (for the 350–1050 nm range) and 2 nm (for the 1050–2500 nm range). The spectral resolution for the FieldSpec Pro is

TABLE 1. Relative moisture estimates employed in plot and quadrat field sampling.[1]

Code	Summary	Description
1	Very dry	Very little moisture, soil does not stick together
2	Dry	Little moisture, soil somewhat sticks together
3	Damp	Noticeable moisture, soil sticks together but crumbles
4	Damp to moist	Very noticeable moisture, soil clumps
5	Moist	Moderate moisture, soil binds, but can be broken apart
6	Moist to wet	Considerable moisture, soil binds and sticks to fingers
7	Wet	Very considerable moisture, water drops can be squeezed out of soil
8	Very wet	Much moisture can be squeezed out of the soil
9	Saturated	Very much moisture, water drips out of soil
10	Very saturated	Extreme moisture, soil is more liquid than solid

[1] Source: Edwards et al., 2000.

3 nm at 700 nm and 10 nm at 1400 and 2100 nm (Analytical Spectral Devices, 2006). For each spectral sample, an 8˚ field of view (FOV) foreoptic was used to record spectral data for an area approximately 10 cm in diameter (with foreoptic mounted at 0.6 m above the area of interest). Radiometric sampling in the field can be logistically difficult, with factors such as battery life, sun location, sky conditions, and travel distance affecting the number of samples that can be collected at a given time and in a given season. Spectral data were recorded for a total of 18 quadrats from seven study plots. For each of these 18 quadrats, we calculated spectral reflectance measurements by averaging a total of 250 individual samples to provide one spectral response curve ranging from visible to mid-infrared wavelengths (350–2500 nm). Spectra were collected for surface-cover types that exhibited uniform or homogeneous composition and often included a number of plant species. These spectra were representative of the vegetation communities and species composition for the 12 plots studied. Each spectral sample was located in the middle of a quadrat (0.25 m²) where percent cover had been estimated.

Remote Sensing Data Preprocessing

To determine the reflectance spectra of a material with a portable spectro-radiometer, two measurements are required in sequence: (i) the spectral response of a calibrated reference panel (Spectralon Reflectance Target calibrated for an 8˚ foreoptic by Labsphere®, Sutton, N.H., 15 October 1999) with near 100% reflectance across the spectrum; and (ii) the spectral response of the target material. Reflectance spectra are calculated by dividing the spectral response of the target by that of the calibrated reference panel. The derivation of this ratio compensates for parameters that are multiplicative in nature and present in both spectral response measurements. Reflectance spectra were collected during clear sky conditions and as close to solar noon as possible.

All satellite data were collected during 23–27 July 2001 between 17:56 and 18:39 UTC, allowing all imagery to be captured at similar solar zenith angles (within 1˚). This method minimized spectral differences due to topographic shading and facilitated a more direct comparison of spectral relationships between the surface and satellite sensors (Thenkabail, 2004). IKONOS multispectral data (4 m spatial resolution) were acquired pre-processed with a 2 m horizontal metric accuracy (Space Imaging Inc., 2006). In order to cover the entire study site, two separate IKONOS overpasses (23 July and 27 July 2001) were required. Landsat 7 ETM+ data (30 m spatial resolution) were collected for the study area on 25 July 2001. All image data were converted to at-satellite exo-atmospheric reflectance, a temporally comparable surface reflectance factor (Moran et al., 2001), following procedures outlined by NASA (2002) and Taylor (2005). Furthermore, the Landsat 7 ETM+ data were georeferenced to the same planimetric database as the IKONOS data (i.e., Universal Transverse Mercator, zone 15N, North American Datum 1983) with an overall root-mean-square (rms) error of approximately 8 m.

Vegetation Index Calculation (NDVI)

Surface spectral reflectance measurements acquired for the 18 selected quadrats were converted to mean values for each wavelength using software from Analytical Spectral Devices (ASD ViewSpecPro, Section 2.2). Surface spectral values for each quadrat were then averaged to correspond to the range of Landsat 7 ETM+ red (630–690 nm) and NIR (780–900 nm) wavelengths. This procedure ensures that the surface spectra correspond to image bandwidths and that the wavelength ranges used in vegetation index calculations are comparable. IKONOS and Landsat 7 ETM+ have identical bandwidths for the red portion of the electromagnetic spectrum and similar ranges for the NIR (i.e., high correlation; R = 0.998, $p < 0.0001$).

The NDVI has been the most commonly applied spectral index for characterizing the vegetation of Arctic environments using various satellite sensors. It is calculated as follows:

$$NDVI = \frac{nir - red}{nir + red} \qquad [1]$$

where nir = near infrared reflectance and red = visible red reflectance.

The 12 study plots were purposely selected to provide a range of exposed soil expanses and soil conditions, i.e., moisture and organic content (Table 2, Fig. 2). These variations were desirable for evaluating how well the NDVI could characterize differing vegetation communities. NDVI values were calculated for plot-level spectra (averaged to correspond to 100 m × 100 m study plot dimensions) using surface spectral measurements and remotely sensed data (i.e., spectro-radiometer, IKONOS, and Landsat 7 ETM+) to compare results from varying spatial resolutions (i.e., measurement scales).

TABLE 2. Approximate habitat types used to characterize study plots.[1]

| Study Plot	Habitat Code	Habitat Description
P1	3	Wet meadows
P2	2	Mesic zonal sites
P3	3	Wet meadows
P4	2	Mesic zonal sites
P5	4b	Snowbeds (poorly drained, later melting)
P6	4a	Snowbeds (well-drained, early melting)
P7	4a	Snowbeds (well-drained, early melting)
P8	3	Wet meadows
P9	5	Streamside sites
P10	3	Wet meadows
P11	4a	Snowbeds (well-drained, early melting)
P12	1	Dry exposed ridges

[1] After Walker, 2000:29.
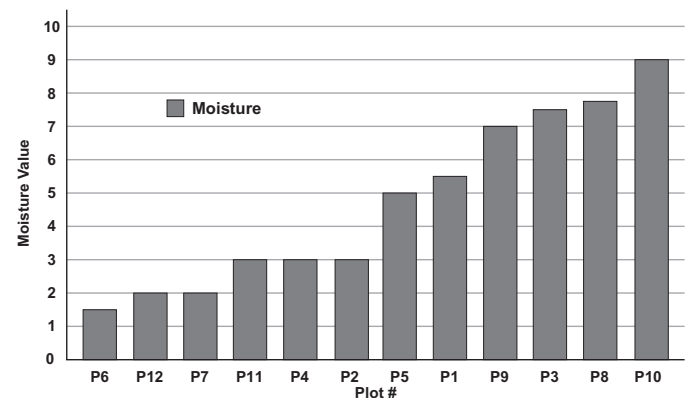
FIG. 2. Moisture estimates for the 12 study plots (P1 to P12), ordered from driest (P6) to wettest (P10).

RESULTS

Surface Moisture and Percent Cover

The plot-level median soil moisture values derived for each plot are presented in Figure 2. To emphasize the range of values observed, the plots are arranged along a gradient from driest to wettest. Results of the moisture estimates show P6 to be the driest site (moisture value < 2; dry to very dry), while P10 is the wettest community (moisture value > 8; very wet to saturated). The plots follow an idealized meso-topographic moisture gradient described by Walker (2000), which allows each plot to be characterized as one of the five major habitat types (Table 2). To reflect these plot moisture regimes, presentations of plot percent cover and NDVI are arranged according to this environmental gradient.

Plot percent cover estimates include all vegetation functional groups, vascular and non-vascular, as well as non-vegetated cover (Fig. 3). The number of forbs present was a determining factor in taxon richness (Fig. 4). *Saxifraga oppositifolia* is most prominent on dry and mesic plots, while a variety of *Pedicularis* spp. may be found on moist to wet sites. However, most community types exhibited a few dominant species (which corresponded to greater
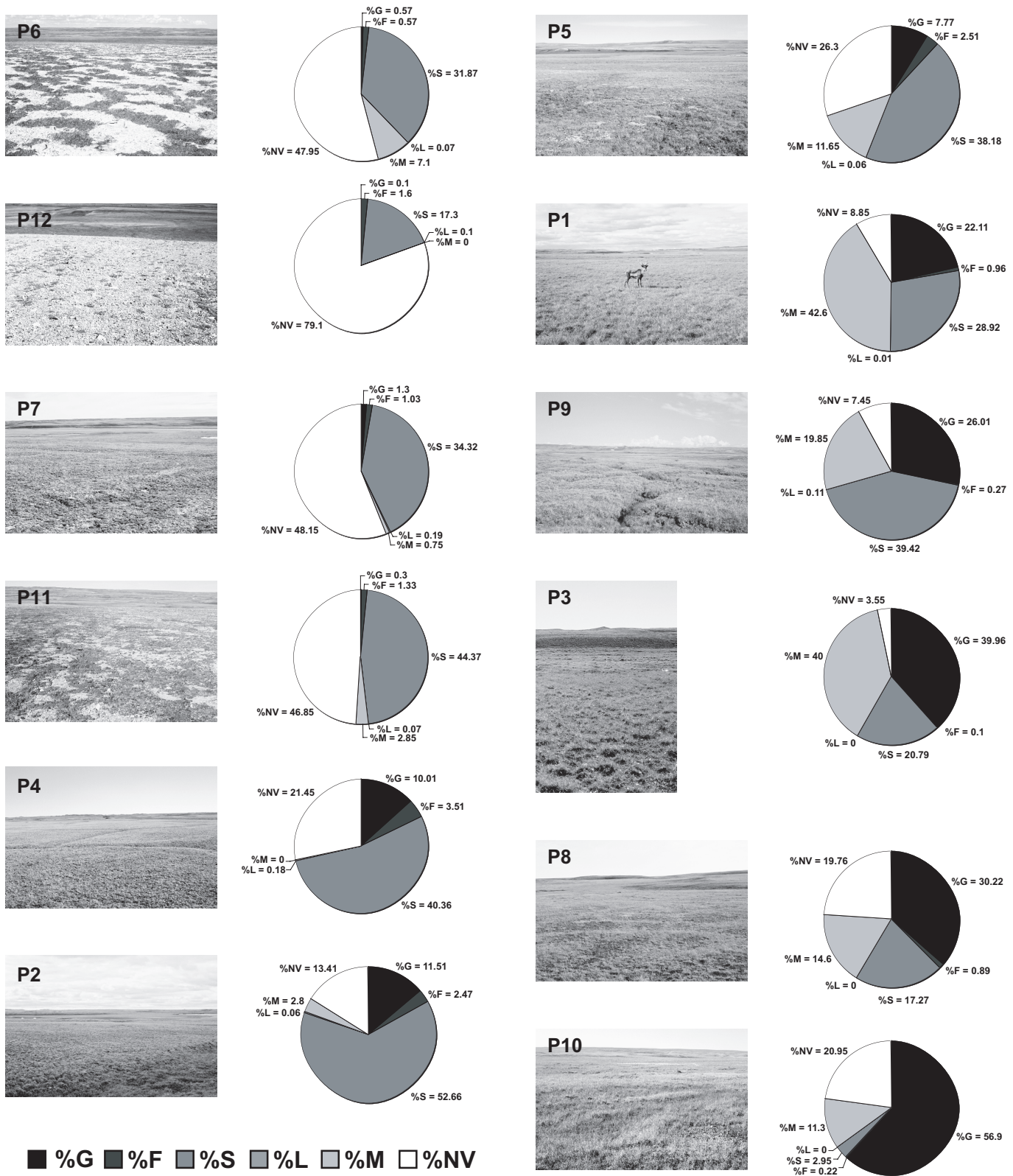
FIG. 3. Photos of vegetation study plots, ordered from driest to wettest (from top left, descending), and percent cover estimates for forbs (%F), graminoids (%G), lichens (%L), mosses (%M), shrubs (%S), and nonvegetated areas (%NV) in each plot.

percent cover), regardless of total species present. On drier plots, like P6, P7, and P12, non-vegetated areas dominate the community, while shrubs (i.e., *Dryas integrifolia* and prostrate *Salix* spp.) contribute the most to vegetation

cover (Fig. 3). As plot moisture increases (P2, P4, P5, and P11), shrubs tend to be the dominant cover type, with an increasing presence of graminoids and forbs, while non-vegetated ground continues to contribute about one-fourth
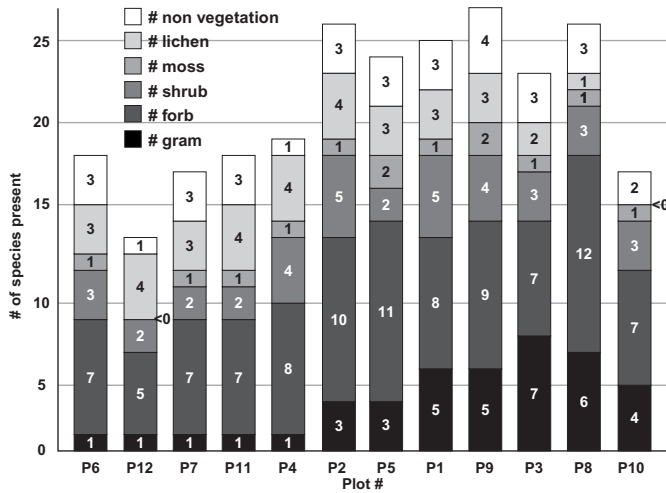
FIG. 4. Estimate of species richness for each plot, indicating the number of species present from each plant functional type.

FIG. 5. NDVI values for the 12 study plots, calculated with data from surface (Su), IKONOS (Ik), and Landsat (La) sensors.

of percent cover (Fig. 3). As plot moisture continues to increase, as in P1, P3, P8, P9, and P10, graminoids (i.e., *Eriophorum* spp. and *Carex* spp.) or bryophytes (i.e., *Sphagnum* spp.) or both become dominant (Fig. 3). Non-vegetated cover does not disappear in wet plots, but its characteristics are much different (i.e., dark, absorbent, open organic materials compared to the rocky, bare soil, or sandy exposed surfaces on dry plots). Lichens are listed in many percent cover estimates, but since they often consti-tute less than 1% of the total, they are not apparent in plot-level percent cover graphic summaries for any community type encountered within the study site (Fig. 3).

NDVI – Surface, IKONOS, Landsat 7 ETM+

Although there are variations, plot NDVI values for each of the remote sensing data sets generally follow a similar trend, in that they increase along the environmental gradient from the driest (i.e., barren) to the wettest (i.e., highly vegetated) sites (Fig. 5). Pearson correlation coef-ficients (R) were calculated to compare the extent to which the surface and satellite (IKONOS and Landsat 7 ETM+) NDVI values are "proportional" to each other across the sampled plots. All three sensors produced NDVI values that are highly correlated, with IKONOS and Landsat 7 ETM+ having the highest correlation (R = 0.98, $p < 0.001$). Similar high correlations were found between surface spectra and Landsat values (R = 0.96) and surface spectra and IKONOS values (R = 0.94) ($p < 0.001$).

The NDVI was calculated for surface spectra converted to mean plot values. It is not surprising that P12 demon-strates the lowest NDVI value (0.15), since it is the site where non-vegetated cover dominates (Figs. 3 and 5). The highest NDVI value (0.61) is found in P9 and P3. The wettest areas are plots P8 (surface NDVI of 0.60) and P10 (surface NDVI of 0.57). While plots P4, P6, P7, and P11 have similar vegetation cover (low-lying shrub cover in-terspersed with rocks and pebbles), the variations in veg-
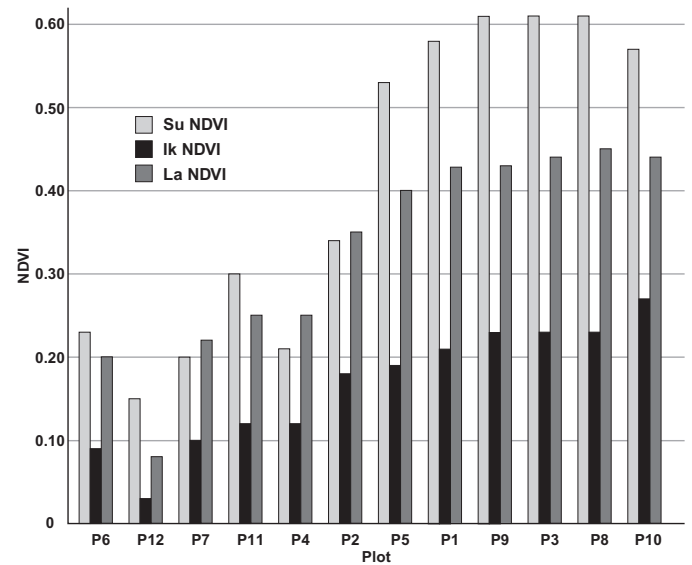
etation density or exposed soil or both (Fig. 3) may ac-count for the varying NDVI values, from 0.2 to 0.3 (Fig. 5).

Plot NDVI comparisons show that Landsat 7 ETM+ NDVI values tend to be lower than surface NDVI values (with the exception of P7 and P4), and the IKONOS NDVI values are the lowest of all the sensors. Furthermore, Landsat 7 ETM+ and IKONOS NDVI values seem to minimize the differentiation between all study plots (Fig. 5). In other words, the similarities between plots reduce the original 12 plots to a loosely defined threefold grouping (NDVI values from Landsat 7 ETM+): i) NDVI ≈ 0.08 (P12); ii) NDVI ≈ 0.20–0.25 (P4, P6, P7, P11); and iii) NDVI ≈ 0.35–0.45 (P2, P5, P1, P3, P9, P8, P10).

Estimating Percent Cover

Bivariate regression analyses were performed to de-termine relationships between percent cover and NDVI values. A strong, significant linear relationship exists between percent cover and the NDVI value for each of the spectral data sets: $R^2 = 0.72$ for IKONOS, 0.74 for surface spectra, and 0.78 for Landsat ETM+ (Fig. 6). Despite the unavoidable shortcomings of a small sample (12 one-hectare study plots), regression analysis remains a valu-able tool for investigating relationships between tundra biophysical variables because very strong relationships can still be determined with relative certainty (Hair et al., 1998). Therefore, highly significant results would sug-gest that more intensive research is warranted to validate these relationships under more extensive sampling. Al-though the vegetation index would usually be considered a function of vegetation amount, scatter plots and regres-sion equations were constructed with the NDVI value as the independent variable in order to calculate percent cover images from the NDVI results (after Shippert et al., 1995).
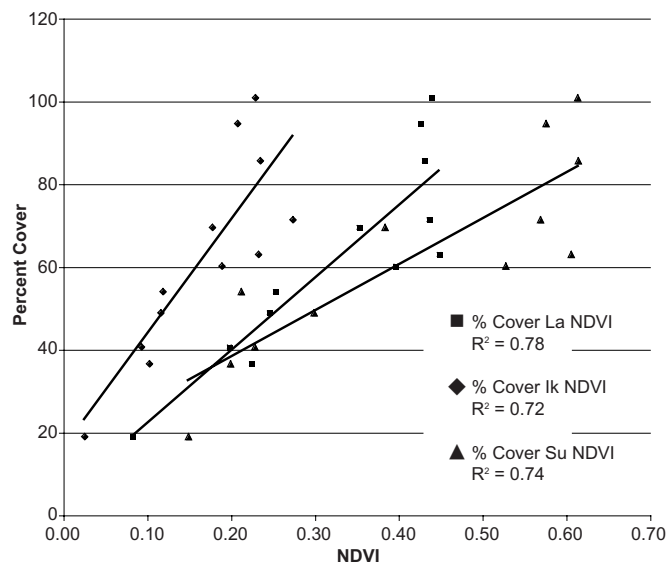
FIG. 6. Linear relations between percent cover and NDVI values for surface (Su), IKONOS (Ik), and Landsat (La) sensors.

DISCUSSION

Moisture and Percent Cover Field Estimates

In the majority of Arctic locations, the environmental factor most closely correlated with vegetation type is soil moisture (Oberbauer and Dawson, 1992). In areas of high elevation, water is a limiting factor and an important determinant of vegetation structure, productivity, and composition; in lower areas, these aspects may not be controlled directly by soil moisture, but rather by factors correlated with or affected by soil moisture, such as nutrient availability, thaw depth, soil aeration, redox potential, and pH (Oberbauer and Dawson, 1992). Micro-scale moisture gradients (across a few metres), such as those in periglacial features (troughs to high-centre polygons, frost boils, or stone stripes) or from wet meadows to beach ridges, have great influence on the pattern and distribution of vegetation throughout tundra plant communities. This within-plot variability is prominently demonstrated in P6, P5, P8, and P9, where small variations in moisture—and frost action—determine the distribution of abundant vegetation as well as exposed, non-vegetated surfaces (Fig. 3). Meso-scale soil moisture has an inverse relationship with slope and elevation: fell-field ridge tops are the driest environments, and moisture increases moving downhill to riparian zones in valleys, which are the wettest habitats (e.g., Table 2, Figs. 2 and 3) (Oberbauer and Dawson, 1992).

Vegetation cover characteristics follow micro-topographic gradients, which influence soil moisture, nutrient availability, snow cover, exposure, and microclimate differences that define habitats broadly as dwarf-shrub heath or moist to wet sedge meadows. Therefore, results presented for plot percent cover estimates (Fig. 3) follow expected trends in vegetation community composition and functional type dominance described in other tundra vegetation research (e.g., Bliss and Matveyeva, 1992; Lloyd et
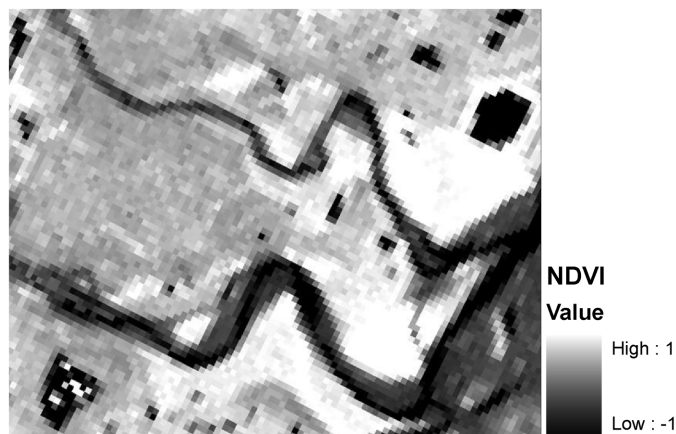
Landsat NDVI Image
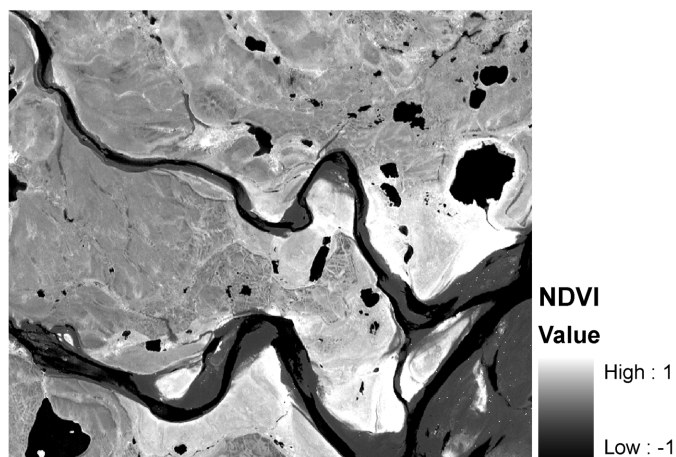
IKONOS NDVI Image

FIG. 7. Landsat (top) and IKONOS (bottom) NDVI images for a sub-area (approximately 6.8 km^2) within the study area (around study plots P1–P3). Dark areas represent regions of low NDVI (-1), while bright areas indicate high NDVI (+1), typically lush green vegetation.

al., 1994; Walker et al., 1994; Murray, 1997; Henry, 1998; Young et al., 1999). The spatial heterogeneity of the study area, regarded as the irregularity of the physical environment that translates into different kinds of plant habitats, demonstrates the importance of local influences on creating a diversity of habitats that can maintain a diversity of species cover (Murray, 1997). These field results are complemented with NDVI calculations (Fig. 5) and evaluations from several different sensor types in order to provide more direct comparisons with other Arctic biophysical remote sensing studies. With much of the spatial heterogeneity being derived from micro-scale moisture gradients, higher spatial resolution sensors such as IKONOS (4 m) may prove useful in capturing surface variability.

NDVI Sensor Comparisons

With the NDVI value calculations based on the absolute measurements of at-sensor reflectance, there still exist systematic differences between the NDVI values across the plots (Table 3). Surface NDVI values are the highest and have the largest dynamic range (0.47). This result can

TABLE 3. Average NDVI values for each plot, and compared across spatial resolutions.

Plot	Su NDVI	Ik NDVI	La NDVI
P6	0.23	0.09	0.20
P12	0.15	0.03	0.08
P7	0.20	0.10	0.22
P11	0.30	0.12	0.25
P4	0.21	0.12	0.25
P2	0.38	0.18	0.35
P5	0.53	0.19	0.40
P1	0.58	0.21	0.43
P9	0.61	0.23	0.43
P3	0.61	0.23	0.44
P8	0.61	0.23	0.45
P10	0.57	0.27	0.44
Min	0.15	0.03	0.08
Max	0.61	0.27	0.45
Dynamic range	0.47	0.25	0.37
Difference in dynamic range	Su NDVI & Ik NDVI	Ik NDVI & La NDVI	Su NDVI & La NDVI
	0.22	0.12	0.10

be explained, at least in part, by the reduced atmospheric path radiance experienced by these ground measures, which gives rise to better contrast between reflectance of visible and near-infrared wavelengths.

IKONOS NDVI values are lower than Landsat 7 ETM+ values, a pattern which is consistent with other studies, in that IKONOS sensors produce higher reflectance in the red band and lower reflectance in the near-infrared band compared to Landsat 7 ETM+ sensors (Goward et al., 2003; Song, 2004). Several other factors may also contribute to the difference. First, the images were collected over a four-day period. Changes to the vegetation cover would be very minimal over this period, but different atmospheric conditions between days can significantly change the NDVI values (Song and Woodcock, 2003). Without in situ atmospheric aerosol data at the times of image acquisition, we cannot perform rigorous atmospheric corrections. Second, band-pass differences between the sensors from the two satellites may contribute to the difference in NDVI values (Song, 2004). Finally, surface bidirectional reflectance can affect NDVI values for the two images. Although the solar zenith and azimuth angles are very similar (within 1°), the off-nadir viewing angles for the IKONOS data are quite different from the nadir view of the Landsat 7 ETM+ data. The difference in viewing angles can cause systematic differences in remotely sensed data (Song and Woodcock, 2003). It remains a major challenge in remote sensing to remove noise from image acquisition on the basis of the various physical factors described above (Song, 2004). Jiang et al. (2006) have suggested that for heterogeneous surfaces, spatial resolution may have an important impact on NDVI measurement, and that NDVI at different resolutions may not be comparable in dark soil backgrounds or with the presence of shadow. In this mid-Arctic ecosystem, soil background reflectance tends to be very high (i.e., red and NIR reflectance ~ 0.3) and shadow is minimal, given the very low vertical structure of the vegetation. Jiang et al. (2006) concluded that in a bright soil, low shadow environment there was no significant difference between NDVI values from coarse- and fine-resolution measurements. Overall, the NDVI values from IKONOS and Landsat ETM+ are very highly correlated, but they have modest differences in their dynamic ranges (0.12) (Table 3; Fig. 5). These values are similar to those from other studies, which concluded that the two sensors were comparable and could be successfully integrated in various ecosystems (Thenkabail, 2004).

Although spatial trends of NDVI values are similar between IKONOS and Landsat 7 ETM+, IKONOS proves more useful in delineating tundra vegetation components because of its superior 4 m spatial resolution (compared to 30 m for Landsat 7 ETM+). Therefore, IKONOS data can detect microsite variations within plots, as well as resolve narrow, local-scale linear and convoluted topographic features (e.g., water-tracks and snowbed vegetation—usually the most productive communities with the highest NDVI values) more precisely than Landsat 7 ETM+ (Fig. 7). For example, the study plots are represented by approximately 625 pixels in an IKONOS image, while in a Landsat 7 ETM+ image they are represented by approximately 9 pixels, depending on plot boundary orientation. However, while IKONOS delineates microsite variations more effectively, there is also potential for enhanced spectral signal confusion at the plot level. This is another important reason to incorporate the use of the NDVI, or similar spectral indices, to ensure more consistent and accurate delineation of vegetation community type as related to percent cover.

Estimating Percent Cover

Stow et al. (1993) found a significant linear relationship between percentage-shrub cover and NDVI values, while Shippert et al. (1995) showed strong linear relationships between NDVI and leaf area index (LAI) values when data were grouped into physiognomic categories. Walker et al. (1995) also suggest that vegetation cover is strongly linked to NDVI values, as well as to other related features, such as landscape age and soil pH. Regression results were
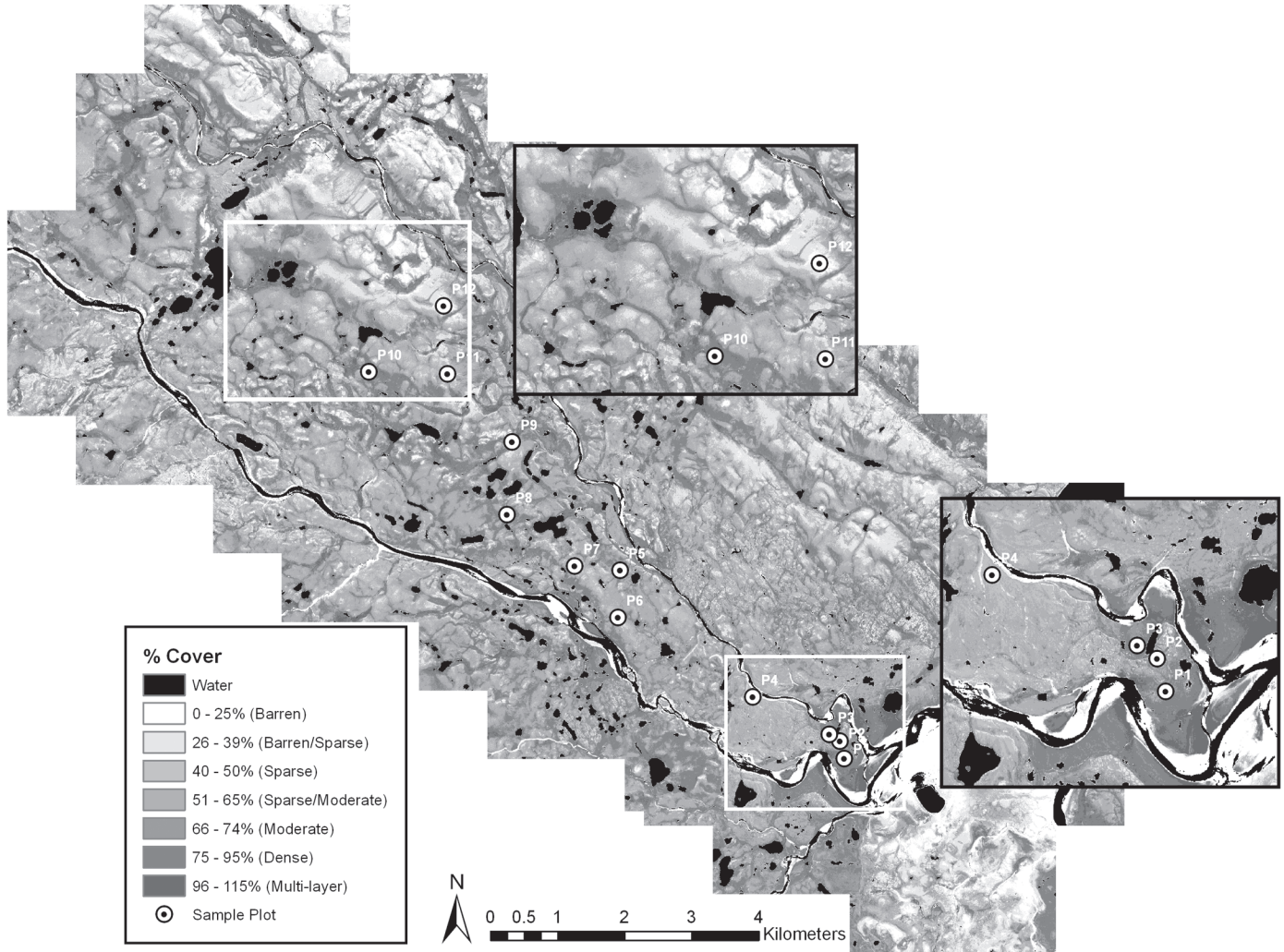
FIG. 8. Image of percent cover from IKONOS NDVI, calculated from the following regression equation: $Y = 275.5 (IK\_NDVI) + 16.07$ ($R^2 = 0.716$, $p < 0.01$).

linear, significant, and consistent across scales (i.e., $R^2 = 0.72-0.78$; $p < 0.01$) (Fig. 6), corroborating trends reported in other Arctic environments.

An image of percent cover derived from the IKONOS NDVI data is presented in Figure 8, which portrays the relationship between percent cover variations (Fig. 3), topographic trends (Table 2), and associated moisture regimes (Fig. 2). Percent cover increases along declining elevations and slopes as a reflection of increased vegetation canopy density in areas of high moisture (i.e., water-tracks, drainage channels, and areas with moderate to minimal exposure). Modeling percent cover over the entire study site provides an interesting perspective on overall vegetation distribution and cover characteristics that would otherwise be difficult to visualize. Although these values must be interpreted with caution (i.e., IKONOS NDVI explains 72% of the vegetation cover variance for the study plots), they provide important preliminary results. Stow et al. (1993) suggest that data with high spatial resolution (i.e., < 10 m) would strengthen NDVI correlations to biophysical variables, making it easier to i) identify

the initial conditions for patch-scale models by inventorying landscape conditions and their relative proportions; ii) stratify landscapes into relatively homogeneous response units for spatially distributed modeling of material and energy transport; iii) extrapolate model simulations by mapping areas that are potentially sensitive to particular disturbances; and iv) assess landscape- and regional-scale model simulations by comparative spatial pattern analyses. Here, coefficients of determination for NDVI and percent cover were very similar for the IKONOS and Landsat data. This similarity is a function of averaging the IKONOS NDVI data to the plot level for correlation analysis. However, applying the model to the high-resolution data provides a more precise definition of the variability in vegetation percent cover across the landscape. IKONOS data therefore show tremendous potential for tundra vegetation mapping at local scales: they are able to delineate percent cover trends and microsite variability throughout the study area (Fig. 8). At the same time, similarly accurate estimates of percent cover can be derived from Landsat data at intermediate or regional scales.

CONCLUSIONS

Remote sensing is a valuable and integral tool for characterizing vegetation communities throughout the Arctic and in evaluating regional changes in tundra vegetation composition or distribution. Furthermore, spectral vegetation indices such as the NDVI play an important role in modeling biophysical variables over large expanses of land on the basis of spectral reflectance. Reflectance data and related biophysical variables cannot easily, or frequently, be collected through field studies in Arctic regions. In this study, NDVI values were calculated using surface spectroradiometer, IKONOS, and Landsat 7 ETM+ data.

Linear regression analyses demonstrated strong, significant relationships between NDVI and percent cover (i.e., $R^2 > 0.7$, $p < 0.01$) for each of the sensor types (i.e., spatial resolutions). IKONOS data were used to extrapolate plot-specific results across the entire study area. While modeling of percent cover in this manner must be interpreted with caution, it is encouraging that the results tend to delineate the environmental gradients that were observed during the field campaign. These results establish initial estimates upon which to build and improve the accuracy of spatial and spectral representation of tundra biophysical variables on the Boothia Peninsula and throughout the Arctic.

The utility of high-resolution multispectral data (e.g., IKONOS data) has been minimally investigated in Arctic environments. Strengthening our understanding of biophysical remote sensing in Arctic environments, while taking advantage of improvements in satellite spatial resolving power, provides enhanced capacity for circumpolar vegetation mapping. In addition, improving our capacity to estimate biophysical variables using remote sensing data will enhance our ability to capture baseline vegetation and environmental information, while allowing for the monitoring of environmental change. Remote sensing research efforts are continuing at this site and have been expanded along a latitudinal gradient to include Cape Bounty, Melville Island, Nunavut. Their goal is to i) characterize and classify vegetation communities; ii) model soil moisture, fraction of vegetation cover and biomass across vegetation communities; and iii) link remote sensing derivatives (such as NDVI values) with vegetation community types for modeling of carbon dioxide flux.

ACKNOWLEDGEMENTS

REFERENCES

ANALYTICAL SPECTRAL DEVICES. 2006. FieldSpec Pro FR Specs. Boulder, Colorado: Analytical Spectral Devices Inc. http://www.asdi.com/products_specifications-FS3.asp.

BARBOUR, M.G., BURK, J.H., and PITTS, W.D. 1987. Terrestrial plant ecology. Menlo Park, California: The Benjamin/Cummings Publishing Company, Inc.

BLISS, L.C., and MATVEYEVA, N.V. 1992. Circumpolar Arctic vegetation. In: Chapin F.S., III, Jeffries, R.L., Reynolds, J.F., Shaver, G.R., Svoboda, J., and Chu, E.W., eds. Arctic ecosystems in a changing climate: An ecophysiological perspective. San Diego, California: Academic Press, Inc. 59–89.

BOELMAN, N.T., STIEGLITZ, M., RUETH, H.M., SOMMERKORN, M., GRIFFIN, K.L., and SHAVER, G.R., 2003. Response of NDVI, biomass, and ecosystem gas exchange to long-term warming and fertilization in wet sedge tundra. Oecologia 135(3):414–421.

DAVIDSON, A., and CSILLAG, F. 2001. The influence of vegetation index and spatial resolution on a two-date remote sensing-derived relation to C4 species coverage. Remote Sensing of Environment 75:138–151.

DUNGAN, J. 1998. Spatial prediction of vegetation quantities using ground and image data. International Journal of Remote Sensing 19(2):267–285.

DYKE, A.S. 1984. Quaternary geology of Boothia Peninsula and northern District of Keewatin, Central Canadian Arctic. Ottawa: Geological Survey of Canada.

EDWARDS, E.J., MOODY, A., and WALKER, D.A. 2000. A western Alaskan transect to examine interactions of climate, substrate, vegetation, and spectral reflectance. Fairbanks: University of Alaska Fairbanks.

ENVIRONMENT CANADA. 2000. Boothia Peninsula Plateau. http://www.ec.gc.ca/soer-ree/English/Framework/NarDesc/Region.cfm?region=20.

———. 2004. Canadian climate normals 1971–2000. http://climate.weatheroffice.ec.gc.ca/climate_normals/index_e.html.

FORBES, A.C. 2003. Hydrological processes across three large middle Arctic watersheds, Boothia Peninsula, Nunavut. MSc thesis, Department of Geography, Queen's University, Kingston, Ontario, Canada.

GOULD, W.A., RAYNOLDS, M., and WALKER, D.A. 2003. Vegetation, plant biomass, and net primary productivity patterns in the Canadian Arctic. Journal of Geophysical Research (Atmospheres) 108(D2):8167, doi:10.1029/2001JD000948.

GOWARD, S.N., DAVIS, P.E., FLEMING, D., MILLER, L., and TOWNSHEND, J.R. 2003. Empirical comparison of Landsat 7 and IKONOS multispectral measurements for selected Earth Observation System (EOS) validation sites. Remote Sensing of Environment 88:80–99.

HAIR, J.F.J., ANDERSON, R.E., TATHAM, R.L., and BLACK, W.C. 1998. Multivariate data analysis. Upper Saddle River, New Jersey: Prentice Hall.

HANSEN, J., RUEDY, R., GLASCOE, J., and SATA, M. 1999. GISS analysis of surface temperature change. Journal of Geophysical Research 104:30997–31022.

HANSEN, J., RUEDY, R., SATO, M., and LO, K. 2005. NASA Goddard Institute for Space Studies and Columbia University Earth Institute, GISS Surface Temperature Analysis, Global Temperature Trends: 2005 Summation. http://data.giss.nasa.gov/gistemp/2005/.

HENRY, G.H.R. 1998. Environmental influences on the structure of sedge meadows in the Canadian High Arctic. Plant Ecology 134(1):119–129.

HOPE, A.S., KIMBALL, J.S., and STOW, D.A. 1993. The relationship between tussock tundra spectral reflectance properties and biomass and vegetation composition. International Journal of Remote Sensing 14:1861–1874.

HOPE, A.S., FLEMING, J.B., VOURLITIS, G., STOW, D.A., OECHEL, W.C., and HACK, T. 1995. Relating CO_2 fluxes to spectral vegetation indices in tundra landscapes: Importance of footprint definition. Polar Record 31:245–250.

JACOBSEN, A., and HANSEN, B.U. 1999. Estimation of the soil heat flux/net radiation ratio based on spectral vegetation indexes in high-latitude Arctic areas. International Journal of Remote Sensing 20:445–461.

JENSEN, J.R. 2007. Remote sensing of the environment: An earth resource perspective. Upper Saddle River, NJ: Prentice Hall.

JIA, G.J., EPSTEIN, H.E., and WALKER, D. 2003. Greening of Arctic Alaska, 1981–2001. Geophysical Research Letters 30(20), 2067, doi:10.1029/2003GL018268.

JIANG, Z., HUETE, A.R., CHEN, J., CHEN, Y., LI, J., YAN, G., and ZHANG, X. 2006. Analysis of NDVI and scaled difference vegetation index retrievals of vegetation fraction. Remote Sensing of Environment 101:366–378.

LAIDLER, G.J., and TREITZ, P. 2003. Biophysical remote sensing of Arctic environments. Progress in Physical Geography 27:44–68.

LÉVESQUE, E. 1996. Minimum area and cover-abundance scales as applied to polar desert vegetation. Arctic and Alpine Research 28:156–162.

LLOYD, A.H., ARMBRUSTER, S.W., and EDWARDS, M.E. 1994. Ecology of a steppe-tundra gradient in interior Alaska. Journal of Vegetation Science 5:897–912.

LOBO, A., MOLONEY, K., CHIC, O., and CHIARIELLO, N. 1998. Analysis of fine-scale spatial pattern of a grassland from remotely-sensed imagery and field collected data. Landscape Ecology 13(2):111–131.

LOYA, W.M., and GROGAN, P. 2004. Carbon conundrum on the tundra. News and Views. Nature 431:406–408.

McFADDEN, J.P., CHAPIN, F.S., and HOLLINGER, D.Y. 1998. Subgrid-scale variability in the surface energy balance of Arctic tundra. Journal of Geophysical Research 103:28947–28961.

McMICHAEL, C.E., HOPE, A.S., STOW, D.A., FLEMING, J.B., VOURLITIS, G., and OECHEL, W. 1999. Estimating CO_2 exchange at two sites in Arctic tundra ecosystems during the growing season using a spectral vegetation index. International Journal of Remote Sensing 20:683–698.

MORAN, M.S., BRYANT, R., THOME, K., NIA, W., NOUVEL-LONA, Y., GONZALEZ-DUGOC, M.P., QI, J., and CLARKE, T.R. 2001. A refined empirical line approach for reflectance factor retrieval from Landsat-5 TM and Landsat-7 ETM+. Remote Sensing of Environment 78:71–82.

MULLER, S.V., RACOVITEANU, A.E., and WALKER, D.A. 1999. Landsat MSS-derived land-cover map of northern Alaska: Extrapolation methods and a comparison with photo-interpreted and AVHRR-derived maps. International Journal of Remote Sensing 20:2921–2946.

MURRAY, D.F. 1997. Regional and local vascular plant diversity in the Arctic. Opera Botanica 132:9–18.

NASA (NATIONAL AERONAUTICS AND SPACE ADMINISTRATION). 2002. Landsat 7 science data user's handbook. http://landsathandbook.gsfc.nasa.gov/hand book.html.

OBERBAUER, S.F., and DAWSON, T.E. 1992. Water-relations of Arctic vascular plants. In: In: Chapin F.S., III, Jeffries, R.L., Reynolds, J.F., Shaver, G.R., Svoboda, J., and Chu, E.W., eds. Arctic ecosystems in a changing climate: An ecophysiological perspective. San Diego, California: Academic Press. 259–279.

OSTENDORF, B., and REYNOLDS, J.F. 1998. A model of Arctic tundra vegetation derived from topographic gradients. Landscape Ecology 13:187–201.

REES, W.G., GOLUBEVA, E.I., and WILLIAMS, M. 1998. Are vegetation indices useful in the Arctic? Polar Record 34:333–336.

ROUSE, J.W., HAAS, R.H., SCHELL, J.A., and DEERING, D.W. 1974. Monitoring vegetation systems in the Great Plains with ERTS. In: Freden, S.C., Mercanti, E.P., and Becker, M.A., eds. Third Earth Resources Technology Satellite-1 Symposium. Proceedings from a conference held 10–14 December 1974 at the National Aeronautics and Space Administration, Scientific and Technical Information Office, Goddard Space Flight Centre, Washington, D.C. 309–317.

SERREZE, M.C., WALSH, J.E., CHAPIN, F.S., III, OSTERKAMP, T., DYURGEROV, M., ROMANOVSKY, V., OECHEL, W.C., MORISON, J., ZHANG, T., and BARRY, R.G. 2000. Observational evidence of recent change in the northern high-latitude environment. Climatic Change 46:159–207.

SHIPPERT, M.M., WALKER, D.A., AUERBACH, N.A., and LEWIS, B.E. 1995. Biomass and leaf-area index maps derived from SPOT images for Toolik Lake and Imnavait Creek areas, Alaska. Polar Record 31:147–154.

SONG, C. 2004. Cross-sensor calibration between IKONOS and Landsat ETM+ for spectral mixture analysis. IEEE Geoscience and Remote Sensing Letters 1(4):272–276.

SONG, C., and WOODCOCK, C.E. 2003. Estimating tree crown size from multi-resolution remotely sensed imagery. Photogrammetric Engineering & Remote Sensing 69(11):1263–1270.

SPACE IMAGING INC. (now GEOEYE INC.). 2006. IKONOS imagery products guide. http://www.geoeye.com/products/imagery/ikonos/.

STONEHOUSE, B. 1989. Polar ecology. London: Blackie and Son Limited.

STOW, D.A., BURNS, B.H., and HOPE, A.S. 1993. Spectral, spatial and temporal characteristics of Arctic tundra reflectance. International Journal of Remote Sensing 14:2445–2462.

STOW, D.A., HOPE, A., McGUIRE, D., VERBYLA, D., GAMON, J., HUEMMRICH, F., HOUSTON, S., RACINE, C., STURM, M., TAPE, K., HINZMAN, L., YOSHIKAWA, K., TWEEDIE, C., NOYLE, B., SILAPASWAN, C., DOUGLAS, D.,

GRIFFITH, B., JIA, G., EPSTEIN, H., WALKER, D., DAESCHNER, S., PETERSEN, A., ZHOU, L., and MYNENI, R. 2004. Remote sensing of vegetation and land-cover change in Arctic tundra ecosystems. Remote Sensing of Environment 89:281–308.

TAYLOR, M. 2005. IKONOS planetary reflectance and mean solar exo-atmospheric irradiance. Dulles, Virginia: Space Imaging Inc. (now GeoEye Inc.).

THENKABAIL, P.S. 2004. Inter-sensor relationships between IKONOS and Landsat-7 ETM+ NDVI data in three ecoregions of Africa. International Journal of Remote Sensing 25(2): 389–408.

VIERLING, L.A., DEERING, D.W., and ECK, T.F. 1997. Differences in Arctic tundra vegetation type and phenology as seen using bi-directional radiometry in the early growing season. Remote Sensing of Environment 60:71–82.

WALKER, D.A. 2000. Hierarchical subdivision of Arctic tundra based on vegetation response to climate, parent material and topography. Global Change Biology 6:19–34.

WALKER, D.A., AUERBACH, N.A., and SHIPPERT, M.M. 1995. NDVI, biomass, and landscape evolution of glaciated terrain in northern Alaska. Polar Record 31:169–178.

WALKER, D., GOULD, W.A., MAIER, H.A., and RAYNOLDS, M.K. 2002. The circumpolar Arctic vegetation map: AVHRR-derived base maps, environmental controls, and integrated mapping procedures. International Journal of Remote Sensing 23(21):4551–4570, doi:10.1080/01431160110113854.

WALKER, D.A., RAYNOLDS, M.K., DANIËLS, F.J.A., EINARSSON, E., ELVEBAKK, A., GOULD, W.A., KATENIN, A.E., KHOLOD, S.S., MARKON, C.J., MELNIKOV, E.S., MOSKALENKO, N.G., TALBOT, S.S., YURTSEV, B.A., and the other members of the CAVM team. 2005. The circumpolar Arctic vegetation map. Journal of Vegetation Science 16: 267–282.

WALKER, M.D., WALKER, D.A., and AUERBACH, N. 1994. Plant communities of a tussock tundra landscape in Brooks Range Foothills, Alaska. Journal of Vegetation Science 5: 843–866.

YOUNG, C.G., DALE, M.R.T., and HENRY, G.H.R. 1999. Spatial pattern of vegetation in High Arctic sedge meadows. Ecoscience 6:556–564.